Negative Role of Colony-Stimulating Factor-1 in Macrophage, T Cell, and B Cell Mediated Autoimmune Disease in MRL-*Fas*^{lpr} Mice

Deborah M. Lenda, E. Richard Stanley and Vicki R. Kelley

J Immunol 2004; 173:4744-4754; ;
http://www.jimmunol.org/content/173/7/4744

The Journal of Immunology is published twice each month by
The American Association of Immunologists, Inc.,
9650 Rockville Pike, Bethesda, MD 20814-3994.

Print ISSN: 0022-1767 Online ISSN: 1550-6606.

Negative Role of Colony-Stimulating Factor-1 in Macrophage, T Cell, and B Cell Mediated Autoimmune Disease in MRL-*Fas*^{lpr} Mice[1]

Deborah M. Lenda,* E. Richard Stanley,† and Vicki R. Kelley[2]*

Inflammation in the kidney and other tissues (lung, and salivary and lacrimal glands) is characteristic of MRL-*Fas*^{lpr} mice with features of lupus. Macrophages (Mϕ) are prominent in these tissues. Given that 1) Mϕ survival, recruitment, proliferation, and activation during inflammation is dependent on CSF-1, 2) Mϕ mediate renal resident cell apoptosis, and 3) CSF-1 is up-regulated in MRL-*Fas*^{lpr} mice before, and during nephritis, we hypothesized that CSF-1-deficient MRL-*Fas*^{lpr} mice would be protected from Mϕ-mediated nephritis, and the systemic illness. To test this hypothesis, we compared CSF-1-deficient MRL-*Fas*^{lpr} with wild-type strains. Renal pathology is suppressed and function improved in CSF-1-deficient MRL-*Fas*^{lpr} mice. There are far fewer intrarenal Mϕ and T cells in CSF-1-deficient MRL-*Fas*^{lpr} vs wild-type kidneys. This leukocytic reduction results from suppressed infiltration, and intrarenal proliferation, but not enhanced apoptosis. The CSF-1-deficient MRL-*Fas*^{lpr} kidneys remain preserved as indicated by greatly reduced indices of injury (nephritogenic cytokines, tubular apoptosis, and proliferation). The renal protective mechanism in CSF-1-deficient mice is not limited to reduced intrarenal leukocytes; circulating Igs and autoantibodies, and renal Ig deposits are decreased. This may result from enhanced B cell apoptosis and fewer B cells in CSF-1-deficient MRL-*Fas*^{lpr} mice. Furthermore, the systemic illness including, skin, lung, and lacrimal and salivary glands pathology, lymphadenopathy, and splenomegaly are dramatically suppressed in CSF-1-deficient MRL-*Fas*^{lpr} as compared with wild-type mice. These results indicate that CSF-1 is an attractive therapeutic target to combat Mϕ-, T cell-, and B cell-mediated autoimmune lupus. *The Journal of Immunology,* 2004, 173: 4744–4754.

Inflammation is a central feature in the MRL-*Fas*^{lpr} strain with spontaneous autoimmune disease that mimics human systemic lupus erythematosus (1). Multiple tissues in this strain are targeted for inflammation including kidneys, skin, lungs, glands, and joints. However, most MRL-*Fas*^{lpr} mice succumb to renal failure (1, 2). Macrophages (Mϕ)[3] are notably abundant in the kidneys of MRL-*Fas*^{lpr} mice, and following activation mediate renal destruction. Mϕ that accumulate in the kidney during inflammation are activated, as reflected by their increased expression of Ia, and enhanced generation of IFN-γ, TNF-α, and reactive oxygen species (3–6). We have established that activated Mϕ initiate renal resident cell apoptosis (6, 7). Therefore, we reason strategies that prevent Mϕ recruitment, proliferation, and activation will obviate inflammation and the tissue destruction in the MRL-*Fas*^{lpr} strain.

CSF-1 is a chemotactic survival and proliferation factor for Mϕ that is produced by a variety of renal resident cells including tubular epithelial cells (TEC), mesangial cells, and fibroblasts (8–10). CSF-1 is closely linked to the pathogenesis of lupus nephritis in MRL-*Fas*^{lpr} mice. This is based on our prior findings that 1) CSF-1 in the serum and CSF-1 mRNA transcripts in the kidney cortex are evident in advance of overt renal pathology in MRL-*Fas*^{lpr} mice, and continue to rise with advancing nephritis (11, 12); 2) renal resident cells, in particular TEC, are a primary source of CSF-1 in the kidney (13, 14); 3) gene transfer of CSF-1 into the kidney of *lpr* strains recruits Mϕ and autoreactive T cells, thereby initiating nephritis (15); 4) intrarenal CSF-1 production is dependent on a stimulant in the circulation of MRL-*Fas*^{lpr} mice with nephritis (12, 13); and 5) CSF-1 recruits and regulates Mϕ proliferation, and is required for Mϕ activation, and in turn, renal resident cell apoptosis (6). Based on this evidence, we hypothesized Mϕ-mediated lupus nephritis, and the systemic illness will be suppressed in MRL-*Fas*^{lpr} mice lacking CSF-1.

The recessive mutation, osteopetrotic (*Csf1*^{op}), is an inactivating mutation in the mouse *CSF-1* gene (16–18). *Csf1*^{op}/*Csf1*^{op} mice are CSF-1-deficient (17, 18). To eliminate CSF-1 in the MRL-*Fas*^{lpr} strain, we introduced the *Csf1*^{op} mutation onto the MRL-*Fas*^{lpr} background and generated *Csf1*^{op}/*Csf1*^{op} mice by breeding. We now report that CSF-1-deficient MRL-*Fas*^{lpr} mice are protected from lupus nephritis, and the systemic illness. We have determined that CSF-1 has a broad spectrum of actions in the MRL-*Fas*^{lpr} strain. CSF-1 mediates Mϕ, T cell, and B cell functions that are instrumental in the pathogenesis of in MRL-*Fas*^{lpr} mice. Taken together, CSF-1 is a potential therapeutic target to combat lupus nephritis, and the systemic illness in humans.

Materials and Methods

Mice

MRL/MpJ-*Fas*^{lpr}/*Fas*^{lpr} (MRL-*Fas*^{lpr}), C57BL/6J, and osteopetrotic (*Csf1*^{op}/*Csf1*^{op}) mice and littermate control (+/*Csf1*^{op} or +/+) mice on the

*Laboratory of Molecular Autoimmune Disease, Renal Division, Brigham and Women's Hospital, Harvard University Medical School, Boston, MA 02115; and †Department of Developmental and Molecular Biology, Albert Einstein College of Medicine, Bronx, NY 10461

Received for publication April 1, 2004. Accepted for publication July 28, 2004.

The costs of publication of this article were defrayed in part by the payment of page charges. This article must therefore be hereby marked *advertisement* in accordance with 18 U.S.C. Section 1734 solely to indicate this fact.

[1] This work was supported in part by National Institutes of Health Grants 1F32DK-6029101 (to D.M.L.), DK-36149, DK-56848, and DK-52369 (to V.R.K.), CA32551, CA26504, and 5P30-CA13330 (to E.R.S.), and by a grant from the Alliance for Lupus Research (to V.R.K.).

[2] Address correspondence and reprint requests to Dr. Vicki R. Kelley, Brigham and Women's Hospital, Harvard Institutes of Medicine, 77 Avenue Louis Pasteur, Boston, MA 02115. E-mail address: vkelley@rics.bwh.harvard.edu

[3] Abbreviations used in this paper: Mϕ, macrophage; TEC, tubular epithelial cell; PCNA, proliferating cell nuclear Ag; BUN, blood urea nitrogen; iNOS, inducible NO synthase.

0022-1767/04/$02.00

C57BL/6J × C3Heb/FeJ-a/a background were purchased from The Jackson Laboratory (Bar Harbor, ME). These mice were housed and bred in our pathogen-free animal facility.

Generating CSF-1-deficient MRL-Fas^{lpr} mice

We constructed CSF-1-deficient MRL-*Fas^{lpr}* strain (*Csf1^{op}/Csf1^{op}*; MRL-*Fas^{lpr}*) mice using a backcross-intercross scheme. Both male and female *Csf1^{op}/Csf1^{op}* mice have poor fertility (19, 20). Therefore, heterozygotes were bred to generate a *Csf1^{op}/Csf1^{op}*; MRL-*Fas^{lpr}* strain. MRL-*Fas^{lpr}* mice were crossed with +/*Csf1^{op}* mice to yield a F_1 generation. These F_1 mice were intercrossed and the progeny screened for the *Fas^{lpr}* mutation and *Csf1^{op}* allele by PCR amplification of tail genomic DNA using specific primers (21). MRL mice homozygous for *Fas^{lpr}* and heterozygous for *Csf1^{op}* were backcrossed to MRL-*Fas^{lpr}* mice two more times to generate +/*Csf1^{op}* MRL-*Fas^{lpr}* mice (N3). These mice were intercrossed to generate the *Csf1^{op}/Csf1^{op}*; MRL-*Fas^{lpr}* and the +/*Csf1^{op}*; MRL-*Fas^{lpr}* mice. *Csf1^{op}/Csf1^{op}*; MRL-*Fas^{lpr}* mice, readily identified because they lack incisors, were provided with a powdered form of standard mouse chow.

We evaluated the CSF-1-deficient and CSF-1-intact MRL-*Fas^{lpr}* mice at N3 for several reasons. In experiments in which the *Csf1^{op}* mutation was backcrossed onto C57BL/6J, C3H/HeJ, and FVB/NJ strain for five generations the only viable homozygous mutant progeny obtained with our routine powdered chow and care were on the FVB/NJ strain background. In our initial attempts to introduce the mutation onto the MRL-*Fas^{lpr}* background, we encountered a loss of viability of the *Csf1^{op}/Csf1^{op}* mice at a backcross generation of N4 (our unpublished observation). We attributed this to a loss of modifier genes that enhance survival of CSF-1-deficient mice during the backcrossing. Because our prior studies using wild-type mice of other strains backcrossed to MRL-*Fas^{lpr}* for three generations indicated that their phenotype was similar to the MRL-*Fas^{lpr}* strain (22–24), we evaluated the CSF-1-deficient MRL-*Fas^{lpr}* mice at the N3 backcross generation. Importantly, the lupus susceptibility loci are located on chromosomes 4, 5, 7, and 10 (25) and therefore are expected to segregate independently of the *Csf-1* gene located on chromosome 3. Thus, the Csf-1 deficiency mutation can be introduced into MRL-*Fas^{lpr}* mice with minimal effect on the background of disease related genes.

We entered 17 CSF-1-deficient MRL-*Fas^{lpr}* mice and 35 CSF-1-intact MRL-*Fas^{lpr}* mice into the protocol. We evaluated nearly equal proportions of females and males in the CSF-1-deficient and -intact MRL-*Fas^{lpr}* strains (55 and 63%, respectively). In all experiments, we compared equal proportions of females and males in the CSF-1-deficient with intact MRL-*Fas^{lpr}* strains. Because the 50% mortality of the intact MRL-*Fas^{lpr}* mice at the N3 generation is extended by ~2 mo compared with the MRL-*Fas^{lpr}* mice to which they were backcrossed, pathology was evaluated at 6 and/or 8 mo of age.

Histopathology

Renal. We fixed kidneys in 10% formalin for 24 h, and stained paraffin sections (4 μm) with periodic acid Schiff reagent. We evaluated kidney pathology as previously described (26). Briefly, glomerular pathology was assessed by examining 20 glomerular cross-sections (gcs) per kidney and scoring each glomerulus on a semiquantitative scale: 0 = normal (35–40 cells/gcs); 1 = mild (glomeruli with few lesions showing slight proliferative changes, mild hypercellularity (41–50 cells/gcs), and/or minor exudation; 2 = moderate (glomeruli with moderate hypercellularity (51–60 cells/gcs), including segmental and/or diffuse proliferative changes, hyalinosis, and moderate exudates); and 3 = severe (glomeruli with segmental or global sclerosis and/or severe hypercellularity (>60 cells/gcs), necrosis, crescent formation, and heavy exudation). Interstitial/tubular pathology was assessed semiquantitatively on a scale of 0–3 in 10 randomly selected high power fields (×400). We determined the largest and average number of infiltrates and damaged tubules and adjusted the grading system accordingly: 0 = normal, 1 = mild, 2 = moderate, and 3 = maximum. Perivascular cell accumulation was determined semiquantitatively by scoring the number of cell layers surrounding the majority of vessel walls (score: 0 = none; 1 = <5; 2 = 5–10; and 3 = >10).

Other tissues. We fixed lung, salivary glands, and lacrimal glands in 10% formalin for 24 h, stained paraffin sections with periodic acid Schiff reagent and evaluated these tissues by light microscopy as previously reported (26). Perivascular and peribronchiolar leukocyte infiltration were assessed semiquantitatively in 10 random vessels and bronchi, respectively (0 = none; 1 = <3 layers in <50%; 2 = 3–6 cell layers in >50%; 3 = >6 layers in >50%). We scored the salivary gland inflammation on a scale of 0–3 (0 = no inflammatory cells); 1 = few perivascular and periductal inflammatory infiltrates (<100 cells); 2 = moderate number of perivascular and periductal inflammatory infiltrates (100–500 cells); 3 = extensive inflammation with large inflammatory foci (>500 cells). Lacrimal gland inflammation was scored on a scale of 0–3 (0 = no inflammation; 1 = the presence of at least one focus; 2 = multiple foci; 3 = multiple foci plus evidence of gland destruction).

Blood urea nitrogen (BUN)

We evaluated BUN levels using a colorimetric analysis kit (Urea Nitrogen kit; Sigma-Aldrich, St. Louis, MO) according to manufacturer's instructions. A standard curve was generated and used to determine the concentration of urea nitrogen in the serum samples, which were collected when mice were sacrificed.

Circulating monocytes

Blood monocytes were determined by analyzing whole blood on a Hemavet 850 (Drew Scientific, Portsmouth, RI).

Identifying infiltrating cells

Immunostaining. We stained cryostat-sectioned kidney, spleen, lung, and salivary and lacrimal glands (4 μm) for the presence of Mϕ with anti-CD68 Ab (Serotec, Oxford, U.K.), T cells with anti-CD4, anti-CD8, and anti-B220 Ab (BD Pharmingen, San Diego, CA), and B cells with anti-CD19 Ab (BD Pharmingen) using the immunoperoxidase staining method, as previously described (27). Of note, we have previously determined that the B220-positive cells in the MRL-*Fas^{lpr}* kidney are the unique double negative T cells, and are not B cells (22, 28, 29). Interstitial Mϕ and T cells were determined by counting the number of positive cells in 10 randomly selected high-power fields, glomerular Mϕ and T cells were counted in 10 random glomeruli.

Flow cytometry. We dissociated kidneys into single cell suspension using mechanical disaggregation. After removing the capsule, kidneys were placed into a small (2.5 cm^2) 70-μm mesh bag and immersed in 10 ml of PBS. While holding the bag with a pair of forceps, a 1-ml syringe plunger was used to press kidney cells through the mesh bag into the PBS. Cells were collected by centrifugation. RBC were lysed using ACK lysing buffer (BioSource International, Camarillo, CA), and the remaining cells were washed in PBS. FACS buffer (PBS, 5% FBS, and 0.09% NaN_3) was used to wash the cells and dilute Ab. We stained these cells with anti-CD68 Ab-FITC, and either anti-inducible NO synthase (iNOS) Ab (BD Transduction Laboratories, San Diego, CA), anti-CD23 Ab-FITC, or anti-CD69 Ab-FITC (eBiosciences, San Diego, CA) for 30 min and analyzed 10,000 cells using FACSCalibur.

Intrarenal proliferating and apoptotic cells

Proliferating cells. To determine the percentage of proliferating leukocytes and TEC we stained paraffin-embedded kidney sections with proliferating cell nuclear Ag (PCNA; DAKO, Carpinteria, CA). Briefly, kidney sections were deparaffinized in xylene (2 × 15 min) then placed in 100% ethanol and rehydrated in decreasing increments of ethanol. Ag retrieval was performed by placing slides in 10 mM sodium citrate buffer (pH 6) and microwaving on high power for 12 min. PCNA was biotinylated and detected on sections by using ARK kit (DAKO) according to manufacturer's instruction. Proliferating tubules were determined by counting the number of positively stained tubules in 10 randomly selected high power fields. The percentage of proliferating leukocytes was determined by dividing the number of proliferating leukocytes by the total number of infiltrating leukocytes per high power field.

Apoptotic cells. Apoptotic cells were detected in paraffin embedded kidneys by enzymatic in situ labeling of apoptosis-induced DNA strand breaks (TUNEL method) using TdT FragEL DNA Fragmentation Detection kit (Oncogene, Boston, MA) according to the manufacturer's instructions. The number of TUNEL positive cells were counted in 10 random high-power fields, and categorized as either tubular, or infiltrating cells. The percentage of apoptotic leukocytes was determined by dividing the number of apoptotic leukocytes by the total number of infiltrating leukocytes per high-power field.

IgG and C3 deposits within renal glomeruli

To determine IgG and C3 deposits in the kidney, we incubated cryostat-sectioned tissue (4 μm) with 20% normal goat serum, followed by FITC-conjugated goat anti-mouse IgG and FITC-conjugated goat IgG fraction of mouse C3 (Cappel Laboratory, Malvern, PA) as previously described (26). The fluorescence intensity within the peripheral glomerular capillary walls and mesangium were scored on a scale of 0–3 (0 = none; 1 = weak; 2 = moderate; 3 = strong). At least 10 glomeruli per section were analyzed.

Cytokine transcripts in kidney

The expression of MCP-1, IFN-γ, TNF-α, and RANTES was determined in the renal cortex using real-time, two-step quantitative RT-PCR. Total RNA was isolated from snap-frozen kidney cortexes using TRIzol (Invitrogen Life Technologies, Carlsbad, CA). Residual DNA was removed by treatment with 1 U of DNase I (Invitrogen Life Technologies) at room temperature for 15 min followed by inactivation at 65°C for 10 min. Reverse transcription reaction was performed on 1 mg of RNA using an oligo(dT) primer and Superscript II reverse transcriptase (Invitrogen Life Technologies). Relative quantitation with real-time two-step RT-PCR was performed with SYBR Green PCR Reagents (Qiagen, Valencia, CA) and an ABI PRISM 7700 Sequence Detection System (Applied Biosystems, Foster City, CA), according to the manufacturer's instructions. Reactions were performed using 1.0 μl of cDNA at a concentration of 100 ng/ml, in a reaction volume of 25 μl. The PCR consists of HotStar *Taq* activation for 15 min at 95°C, then 40 cycles with heating to 95°C for 15 s and cooling to 60°C for 1 min. The mRNA levels were normalized to those of GAPDH. The PCR primers used were as follows: GAPDH, sense 5′-CAT GGC CTC CAA GGA GTA AG-3′, antisense 5′-CCT AGG CCC CTC CTG TTA TT-3′; IFN-γ, sense 5′-AAC GCT ACA CAC TGC ATC TTG G-3′, antisense 5′-GCC GTG GCA GTA ACA GCC-3′; MCP-1, sense 5′-ACC AGC AAG ATG ATC CCA AT-3′, antisense 5′-TGT CTG GAC CCA TTC CTT CT-3′; TNF-α, sense 5′-TCA GCC GAT TTG CTA TCT CA-3′, antisense 5′-TGG AAG ACT CCT CCC AGG TA-3′; RANTES, sense 5′-TGC CAA CCC AGA GAA GAA GT-3′, antisense 5′-AAG CTG GCT AGG ACT AGA GCA A-3′.

Lymphadenopathy, skin lesions, and splenomegaly

We assessed lymphadenopathy and skin lesions monthly beginning at 2 mo of age. Protruding lymph nodes (cervical, brachial, and inguinal) were palpated and scored on a scale of 0–3 (0 = none; 1 = small, at one site; 2 = moderate, at two different sites; 3 = large, at three or more different sites). Skin lesions were scored by gross pathology: 0 = none; 1 = small (face, ears); 2 = moderate, <2 cm (face, ears, and back); and 3 = severe, >2 cm (face, ears, and back). Splenomegaly was determined at the time of sacrifice by comparing the ratios of spleen to body weight.

Serum Igs

We determined total Ig, IgM, IgG1, IgG2a, IgG2b, and IgG3 isotype by ELISA. Plates were coated overnight at 4°C with goat anti-mouse Ig capture Abs (Southern Biotechnology Associates, Birmingham, AL) in PBS. The wells were blocked for 2 h with 3% BSA/PBS. We added Ig standards to the plate, using a series of 3-fold dilutions, and assessed serum samples using serial dilutions starting at 1/100. Standards and serum samples were incubated overnight at 4°C. Bound Ig was detected with goat anti-mouse detection Abs conjugated with HRP (Southern Biotechnology Associates) and detected with tetramethylbenzidine peroxidase substrate (Kirkegaard & Perry Laboratories, Gaithersburg, MD). The absorbance was measured at 450 nm. In addition, anti-dsDNA Ab isotypes (IgG1, IgG2a, IgG2b, and IgG3) in the CSF-1-deficient MRL-*Fas*^{lpr} and CSF-1-intact MRL-*Fas*^{lpr} mice were determined at five dilutions as previously reported (30).

B cell apoptosis in the bone marrow and spleen

Bone marrow cells were isolated by flushing cold HBSS through the femur and tibia, RBC were lysed with ACK lysing buffer (BioSource International) and the cells resuspended in 5% FBS/PBS. Spleen cells were made into a single cell suspension, RBC were lysed and cells resuspended in 5% FBS/PBS. The number of apoptotic B cells was determined by staining cells to identify B cell markers (CD19 or CD45R/B220) and apoptotic cells (Annexin V^{FITC}; BD Pharmingen). A total of 10,000 cells were analyzed using a flow cytometer.

B cells in the spleen and bone marrow (flow cytometry)

Spleen cells derived from CSF-1-deficient and -intact MRL-*Fas*^{lpr} mice (21 day of age) were prepared as a single cell suspension, the RBC were lysed, and the splenocytes were resuspended in 5% FBS/PBS. We identified B cells by staining splenocytes with anti-CD19-PE (eBiosciences) for 30 min. Cells (10,000) were analyzed using flow cytometry. Bone marrow and spleen cells were isolated and prepared as previously described from CSF-1-intact MRL-*Fas*^{lpr} mice (1 mo of age). B cells in the bone marrow and spleen expressing the CSF-1 receptor (c-*fms*) were detected with CD19-FITC (eBiosciences) and CD115-PE (c-*fms*) (eBiosciences) and analyzed using flow cytometry.

Statistical analysis

Data are presented as mean ± SEM. We determined statistical significance using Mann-Whitney *U* test or Student's *t* test.

Results

*Kidney pathology is suppressed in CSF-1-deficient MRL-*Fas^{lpr} *mice*

Tubular/interstitial, glomerular, and perivascular renal pathology is suppressed in CSF-1-deficient as compared with the CSF-1-intact MRL-*Fas*^{lpr} mice at 6 and 8 mo of age (Fig. 1, *a* and *b*). In the CSF-1-intact MRL-*Fas*^{lpr} kidneys pathology is notable and consists of leukocyte infiltrates in the interstitium and perivascular area, tubular casts, dilation, atrophy and/or necrosis, and glomerular hypercellularity and crescent formation. In contrast, the leukocyte infiltrates, tubular and glomerular pathology are dramatically suppressed in CSF-1-deficient MRL-*Fas*^{lpr} kidneys (Fig. 1, *a* and *b*). However, renal pathology in the CSF-1-deficient MRL-*Fas*^{lpr} strain was not entirely prevented because tubular/interstitial, glomerular and perivascular pathology in CSF-1-deficient MRL-*Fas*^{lpr} mice was greater than in MRL$^{+/+}$ mice with normal kidneys (Fig. 1*a*). Of note, the tempo of renal pathology in the CSF-1-intact MRL-*Fas*^{lpr} strain at the N3 generation was modestly slower than the wild-type MRL-*Fas*^{lpr} strain, confirming that there are sufficient MRL background genes at this generation to evaluate the impact of CSF-1 (Fig. 1*a*).

BUN, an indicator of renal function, is suppressed in CSF-1-deficient MRL-*Fas*^{lpr} mice, as compared with the CSF-1-intact MRL-*Fas*^{lpr} mice at 6 and 8 mo of age (Fig. 1*c*). In the absence of CSF-1, the BUN in MRL-*Fas*^{lpr} did not rise above normal levels (C57BL/6 BUN: 23 ± 2 mg/dl, $n = 7$; dashed line at 8 mo of age). As the CSF-1-deficient MRL-*Fas*^{lpr} mice are oliguric, we were unable to collect adequate amounts of urine in a representative number of mice using metabolic cages or the spot urine technique to evaluate urinary protein, or urine creatinine levels. However, because the glomerular architecture remained histologically normal in the CSF-1-deficient MRL-*Fas*^{lpr} strain, we do not suspect that these mice are proteinuric. Taken together, the CSF-1 deficiency in the MRL-*Fas*^{lpr} strain suppresses nephritis and protects from a loss of renal function.

*Leukocytic infiltrates into the interstitium and glomeruli are suppressed in CSF-1-deficient MRL-*Fas^{lpr} *kidneys*

We have previously determined that Mϕ and T cells but not B cells accumulate in the MRL-*Fas*^{lpr} kidney (22–24). The intrarenal T cells consist of CD4, CD8, and unique B220 bearing cells characteristic of the MRL-*Fas*^{lpr} strain (22–24). Mϕ (CD68) and T cell (CD4, CD8, and B220) accumulation in the interstitium, glomerular, and perivascular regions are dramatically reduced (~90%) in CSF-1-deficient as compared with CSF-1-intact MRL-*Fas*^{lpr} mice (Fig. 2). In fact, the number of leukocytic infiltrates in the CSF-1-deficient MRL-*Fas*^{lpr} kidneys remained similar to those in normal mice (C57BL/6J). Therefore, CSF-1 is required for Mϕ and T cell accumulation in the kidney in the MRL-*Fas*^{lpr} mice.

Reduced intrarenal leukocytes result from decreased infiltration, reduced intrarenal proliferation, and not increased apoptosis

The reduction in leukocytes in the CSF-1-deficient MRL-*Fas*^{lpr} kidneys is primarily the result of a decrease in the infiltration of leukocytes in the kidney. In addition, this decrease is, in part, related to a decrease in the percentage of proliferating leukocytes that are recruited into the kidney. We detected 2 ± 0.3% and 7 ± 1% proliferating leukocytes in CSF-1-deficient and CSF-1-intact MRL-*Fas*^{lpr} kidneys, respectively ($n = 5–6$ per group, $p \leq 0.002$).

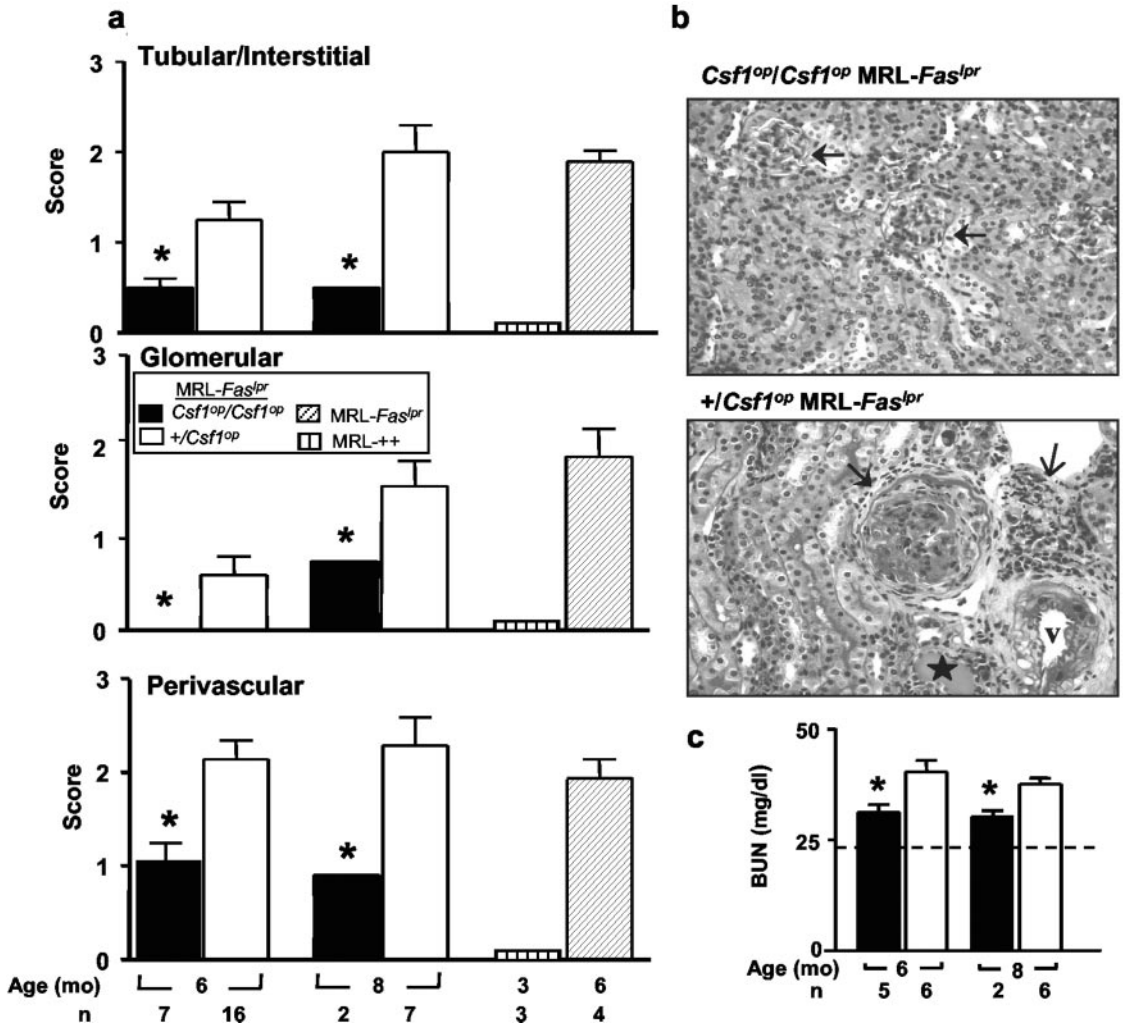

FIGURE 1. CSF-1-deficient MRL-*Fas*^{lpr} mice are protected from kidney disease. *a* and *b*, CSF-1-deficient (*Csf1*^{op}/*Csf1*^{op}) MRL-*Fas*^{lpr}, CSF-1-intact (+/*Csf1*^{op}) MRL-*Fas*^{lpr}, wild-type MRL-*Fas*^{lpr}, and MRL +/+ kidneys were assessed on a scale of 0–3 for tubular damage/interstitial infiltrates, glomerular pathology, and perivascular cell infiltrates by histopathology (periodic acid Schiff stained). *b*, Tubular damage (dilation and cast) (∗), glomerular crescent formation (glomeruli) (filled arrow), and leukocytic infiltration (thin arrow) around the perivascular region (v) is suppressed in CSF-1-deficient MRL-*Fas*^{lpr} mice as compared with CSF-1-intact MRL-*Fas*^{lpr} mice (*a* and *b*). *c*, CSF-1-deficient MRL-*Fas*^{lpr} mice had reduced levels of BUN, as compared with CSF-1-intact MRL-*Fas*^{lpr} mice. Dashed line represents BUN of normal C57BL/6J mice (23 ± 2, $n = 7$). Values are means ± SE; ∗, $p \leq 0.05$, *Csf1*^{op}/*Csf1*^{op} vs +/*Csf1*^{op} MRL-*Fas*^{lpr} mice. Magnification = ×400.

Conversely, the reduction in leukocytes in CSF-1-deficient MRL-*Fas*^{lpr} kidneys was not related to an increase in intrarenal apoptotic leukocytes because the percentage of apoptotic leukocytes in CSF-1-deficient and CSF-1-intact MRL-*Fas*^{lpr} kidneys was similar (4 ± 1% vs 5 ± 1%, respectively, $n = 5$–6 per group, $p \leq 0.72$).

*Fewer activated Mϕ in CSF-1-deficient MRL-*Fas^{lpr} *kidneys*

Activated Mϕ release mediators that induce TEC apoptosis (6, 23). We have established that CSF-1 is required for Mϕ activation during induced renal inflammation (6). Thus, the number of activated Mϕ in the kidney is a gauge for potential renal damage. CSF-1-deficient MRL-*Fas*^{lpr} kidneys have fewer activated Mϕ (CD69, CD23, iNOS) as compared with the CSF-1-intact kidneys at 6 mo of age. The prevention of Mϕ activation was dramatic because the number of activated Mϕ in the CSF-1-deficient MRL-*Fas*^{lpr} kidney did not increase above normal kidney levels (Fig. 3).

*Kidney deposits of Ig and C3 in the glomeruli are diminished in CSF-1-deficient MRL-*Fas^{lpr} *mice*

Glomerular deposits of IgG and C3 are characteristic of nephritis in the MRL-*Fas*^{lpr} strain (31–33). To determine whether CSF-1 alters the deposition of IgG and C3 in the kidney, we evaluated CSF-1-deficient MRL-*Fas*^{lpr} and CSF-1-intact MRL-*Fas*^{lpr} mice at 6 mo of age. The fluorescence intensity of Ig and C3 in the glomerular loops and mesangium was reduced in CSF-1-deficient MRL-*Fas*^{lpr} kidneys (40 and 87%, respectively) as compared with CSF-1-intact MRL-*Fas*^{lpr} kidneys (Fig. 4). Thus, the absence of CSF-1 suppressed the deposition of Ig and C3 within MRL-*Fas*^{lpr} glomeruli.

*Nephritogenic chemokines/cytokines are suppressed in CSF-1-deficient MRL-*Fas^{lpr} *kidneys*

The accumulation of Mϕ and T cells in the kidney is, in part, dependent on key chemoattractant molecules such as MCP-1 and RANTES, which increase during nephritis (23, 34). We determined that MCP-1 and RANTES transcript expression in the renal cortex is suppressed (86 and 89%, respectively) in CSF-1-deficient MRL-*Fas*^{lpr} as compared with the CSF-1-intact MRL-*Fas*^{lpr} mice using real-time PCR (Fig. 5). In fact, the suppression is so profound that MCP-1 and RANTES transcripts do not exceed normal (C57BL/6J) levels (Fig. 5). IFN-γ and TNF-α are nephritogenic

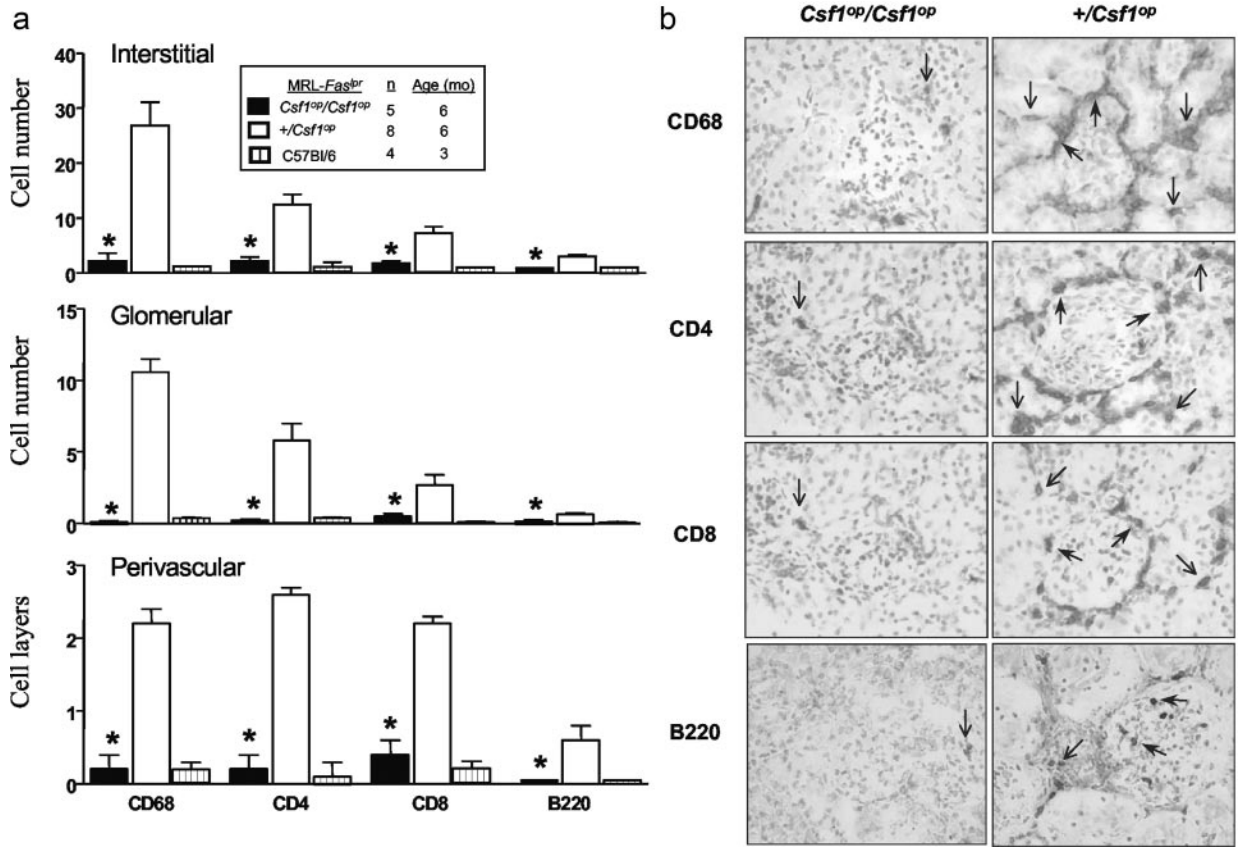

FIGURE 2. Mϕ, CD4, CD8, and B220 T cells are reduced in CSF-1-deficient MRL-*Fas*^{lpr} kidneys. *a*, The number of positive cells in the interstitial, glomerular, and perivascular regions were assessed in CSF-1-deficient and -intact MRL-*Fas*^{lpr} mice at 6 mo of age. *b*, Displays representative photomicrographs of each marker. Glomeruli (filled arrowhead) and interstium (open arrowhead). Values are means ± SE; ∗, $p \leq 0.05$, *Csf1*^{op}/*Csf1*^{op} vs +/*Csf1*^{op} MRL-*Fas*^{lpr} mice. Magnification = ×400.

cytokines that are increased during inflammation in MRL-*Fas*^{lpr} kidneys (35, 36). IFN-γ and TNF-α transcripts are dramatically suppressed and do not rise above normal (C57BL/6J) kidney levels in CSF-1-deficient MRL-*Fas*^{lpr} mice. Of note, MCP-1, RANTES, IFN-γ, and TNF-α transcripts in the +/*Csf1*^{op} MRL-*Fas*^{lpr} and MRL-*Fas*^{lpr} strain are similar (Fig. 5). These data support the concept that in the absence of CSF-1 the progression of MRL-*Fas*^{lpr} autoimmune nephritis is suppressed.

*Suppressed TEC apoptosis and proliferation, indices of pathology, in CSF-1-deficient MRL-*Fas^{lpr} *kidneys*

TEC apoptosis and proliferation are features of TEC injury and repair, respectively (37, 38). We determined that the numbers of apoptotic TEC are decreased (3-fold) in CSF-1-deficient MRL-*Fas*^{lpr} mice as compared with the wild-type strain (Fig. 6*a*). Similarly, the numbers of proliferating TEC are dramatically decreased (6-fold) in CSF-1-deficient MRL-*Fas*^{lpr} mice as compared with the wild-type strain (Fig. 6*b*). Taken together, these findings further support the concept that in the absence of CSF-1 the kidney is spared from injury.

*Systemic pathology, skin lesions, lymphadenopathy, and splenomegaly are suppressed in CSF-1-deficient MRL-*Fas^{lpr} *mice*

CSF-1 has a profound impact on systemic pathology in MRL-*Fas*^{lpr} mice evaluated between 2 and 8 mo of age (Fig. 7). CSF-1-deficient MRL-*Fas*^{lpr} mice are totally spared from skin lesions (Fig. 7*a*, *upper panel*). Similarly, the spleens (spleen per body weight) are considerably smaller in the CSF-1-deficient MRL-*Fas*^{lpr} strain as compared with the CSF-1-intact MRL-*Fas*^{lpr} strain (Fig. 7*b*). In fact, the spleens in CSF-1-deficient MRL-*Fas*^{lpr} mice are not larger than normal (C57BL/6) spleens. Furthermore, lymphadenopathy mainly consisting of an influx of unique T cells (CD4$^-$, CD8$^-$, B220$^+$) into the lymph node (39, 40) is dramatically suppressed in CSF-1-deficient mice as compared with the CSF-1-intact MRL-*Fas*^{lpr} strain (Fig. 7*a*, *lower panel*).

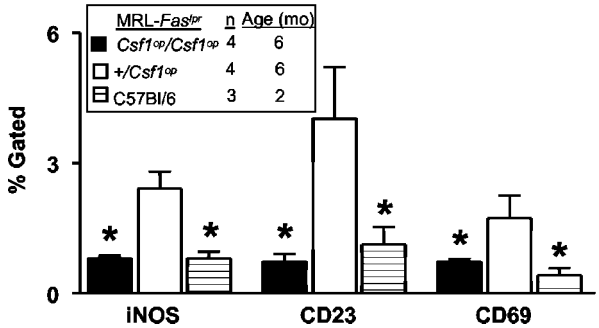

FIGURE 3. Fewer Mϕ in CSF-1-deficient MRL-*Fas*^{lpr} kidneys are activated as compared with Mϕ in CSF-1-intact MRL-*Fas*^{lpr} kidneys. Single cell suspensions were stained for Mϕ (CD68-FITC) and either iNOS, or CD23, or CD69 and analyzed by flow cytometry (10,000 cells were assessed). Activated Mϕ in CSF-1-deficient MRL-*Fas*^{lpr} mice did not increase above normal (C57BL/6 mice). Values are means ± SE; ∗, $p \leq 0.05$, *Csf1*^{op}/*Csf1*^{op} vs +/*Csf1*^{op} MRL-*Fas*^{lpr} mice.

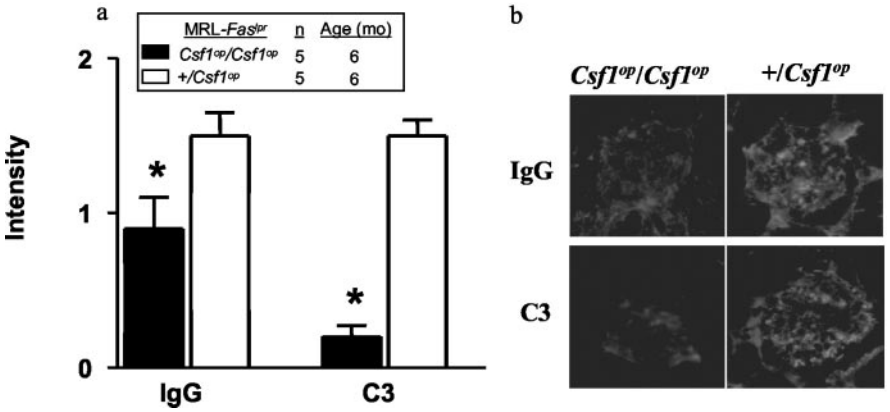

FIGURE 4. IgG and C3 glomerular deposits are suppressed in CSF-1-deficient MRL-*Fas*^{lpr} as compared with wild-type mice (*a*). Representative photomicrographs of IgG and C3 (*b*). Values are means ± SE; ∗, $p \leq 0.05$, *Csf1*^{op}/*Csf1*^{op} vs +/*Csf1*^{op} MRL-*Fas*^{lpr} mice. Magnification = ×400.

*CSF-1-deficient MRL-*Fas^{lpr} *mice have reduced Mϕ, T cells, and B cells in the spleen*

The splenomegaly characteristic of MRL-*Fas*^{lpr} autoimmune disease consists of a huge influx of T cells (unique, CD4, CD8), Mϕ, and B cells (41–44). The numbers of T cells (CD4, CD8, B220), Mϕ (CD68), and B cells (CD19, B220) are reduced in the spleens from the CSF-1-deficient compared with CSF-1-intact MRL-*Fas*^{lpr} mice as evaluated by immunostaining (Fig. 7*c*). Apart from the fact that CD19-bearing B cells are a more mature subset of B220 B cells, B220 is abundantly expressed on the unique T cells in the MRL-*Fas*^{lpr} mice. Because the increase in spleen size is predominantly due to an influx of these unique T cells, the difference between the CD19 and B220 spleen cells is largely a reflection of these unique T cells. The reduction in splenic B cells (CD19) is evident even in CSF-1-deficient MRL-*Fas*^{lpr} as compared with wild-type mice at 21 day of age using flow cytometric analysis (33 ± 6%, $n = 3$ and 47 ± 2%, $n = 11$, respectively; $p \leq 0.03$). The reduction in Mϕ in the spleen is not reflected in the blood because CSF-1-deficient and -intact MRL-*Fas*^{lpr} mice have a similar percentage of blood mononuclear cells (9 ± 1%, $n = 3$ vs 11 ± 1%, $n = 9$, respectively, $p = 0.5$) and CD68-positive cells within the mononuclear cell population (19 ± 3%, $n = 3$ vs 23%, $n = 1$, respectively).

*Leukocyte infiltration into the lung, and salivary and lacrimal glands is suppressed in CSF-1-deficient MRL-*Fas^{lpr} *mice*

Multiple tissues (lung, salivary gland, and lacrimal gland), in addition to kidneys, are targeted for autoimmune destruction in the MRL-*Fas*^{lpr} strain. Lung infiltrates in the MRL-*Fas*^{lpr} mice that are predominately Mϕ (23), accumulate around the perivascular and peribronchiolar region. We determined that the lung

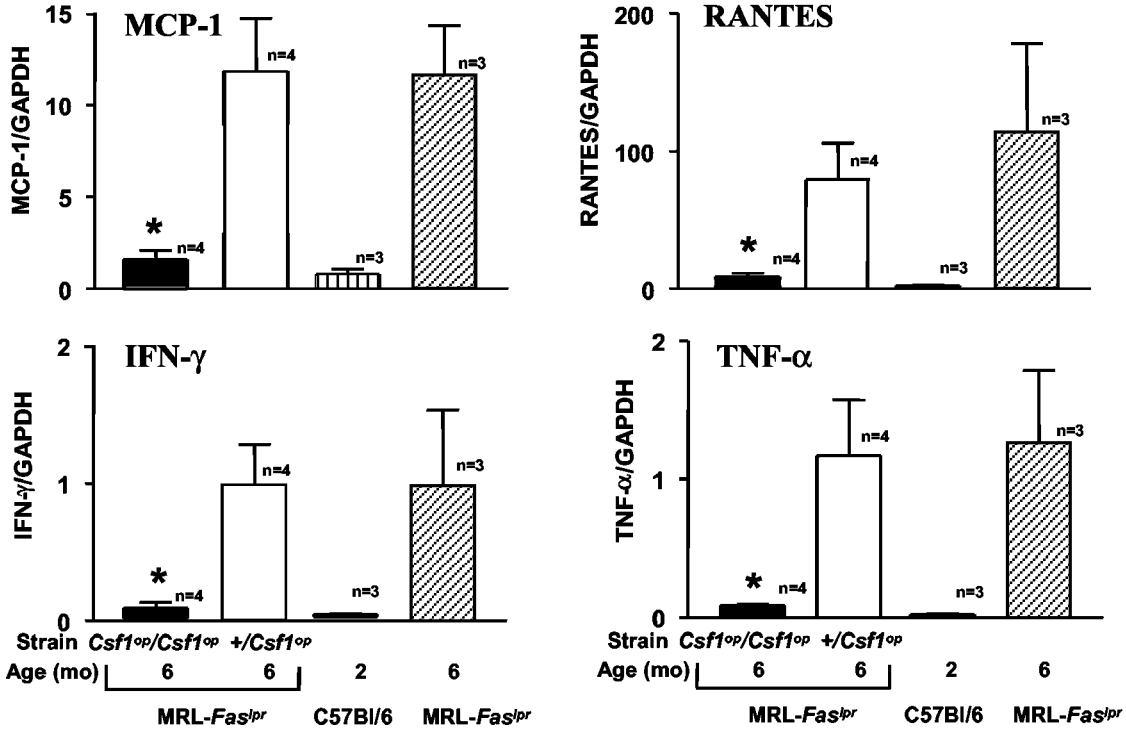

FIGURE 5. Suppressed nephritogenic cytokines in the kidney cortex in CSF-1-deficient MRL-*Fas*^{lpr} mice. MCP-1, RANTES, IFN-γ, and TNF-α expression is suppressed in CSF-1-deficient MRL-*Fas*^{lpr} mice as compared with the wild-type MRL-*Fas*^{lpr} strain at 6 mo of age. Note the increase in nephritogenic cytokines in CSF-1-deficient mice did not rise above normal (C57BL/6J mice), and that the levels in the CSF-1-intact strain were equivalent to those of the MRL-*Fas*^{lpr} mice. Values are means ± SE; ∗, $p \leq 0.05$, *Csf1*^{op}/*Csf1*^{op} vs +/*Csf1*^{op} MRL-*Fas*^{lpr} mice; $p > 0.05$, *Csf1*^{op}/*Csf1*^{op} MRL-*Fas*^{lpr} vs C57BL/6J and +/*Csf1*^{op} MRL-*Fas*^{lpr} vs MRL-*Fas*^{lpr} mice.

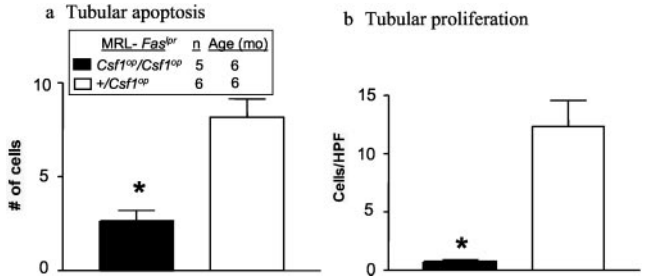

FIGURE 6. Tubular apoptosis and proliferation is suppressed in CSF-1-deficient MRL-*Fas*^{lpr} mice. Increased tubular apoptosis (TUNEL) and proliferation (PCNA), indices of renal injury and repair, are dramatically suppressed in CSF-1-deficient MRL-*Fas*^{lpr} mice (*a* and *b*, respectively). Values are means ± SE; ∗, $p \leq 0.03$, *Csf1*^{op}/*Csf1*^{op} vs +/*Csf1*^{op} MRL-*Fas*^{lpr} mice.

leukocytic infiltrates are drastically reduced (53%) in the CSF-1-deficient as compared with CSF-1-intact MRL-*Fas*^{lpr} mice (Fig. 8*a*). Inflammation in the lacrimal and salivary glands of MRL-*Fas*^{lpr} mice mimics Sjogren's syndrome, a condition resulting in dry eyes and mouth in humans (45). Infiltrating leukocytes are focally distributed within these tissues in MRL-*Fas*^{lpr} mice. We detected a dramatic reduction in leukocytes in the salivary (83%) and lacrimal glands (94%) in CSF-1-deficient MRL-*Fas*^{lpr} mice as compared with the wild-type strain (Fig. 8, *a* and *b*). Thus, the lung and lacrimal and salivary glands pathology is mediated by CSF-1 in the MRL-*Fas*^{lpr} strain.

*Serum Ig isotypes are reduced in CSF-1-deficient MRL-*Fas^{lpr} *mice*

Elevated Igs and Ig class switching is a hallmark of autoimmune disease (46, 47). B cells, responsible for the production of these Abs, are dependent on CSF-1 for survival (48) and differentiation (48, 49). Therefore, we determined whether the protection from autoimmune disease is associated with suppressed circulating Ig isotypes and/or suppressed autoantibodies. Total IgG and IgM isotypes (IgG1, IgG2a, IgG2b, IgG3, and IgM) are highly suppressed in CSF-1-deficient MRL-*Fas*^{lpr} by (79, 73, 75, 100, and 67%, respectively, as compared with the CSF-1-intact MRL-*Fas*^{lpr} mice (Fig. 9*a*). To determine whether there was an alteration in autoantigen-specific serum Ig isotypes, we measured the levels of dsDNA-specific Ig subclasses. CSF-1-deficient MRL-*Fas*^{lpr} mice had reduced levels of serum anti-dsDNA-specific isotypes (IgG1, IgG2a, IgG2b, and IgG3) as compared with CSF-1-intact MRL-*Fas*^{lpr} mice (Fig. 9*b*). Thus, the amount of circulating Ig isotypes and autoantibodies (dsDNA) isotypes in MRL-*Fas*^{lpr} mice are dependent on CSF-1.

*B cell apoptosis in bone marrow and spleen is increased in CSF-1-deficient MRL-*Fas^{lpr} *mice*

We determined that CD19-positive B cells in the bone marrow and spleen of CSF-1-intact MRL-*Fas*^{lpr} mice (1 mo of age) express the CSF-1 receptor assessed by flow cytometry (24 ± 5% and 14 ± 4%, respectively, $n = 3$). Therefore, we tested the hypothesis that B cell survival is altered in CSF-1-deficient as compared with CSF-1-intact MRL-*Fas*^{lpr} mice. Apoptotic B cells in the bone marrow and spleen are increased in CSF-1-deficient MRL-*Fas*^{lpr} mice

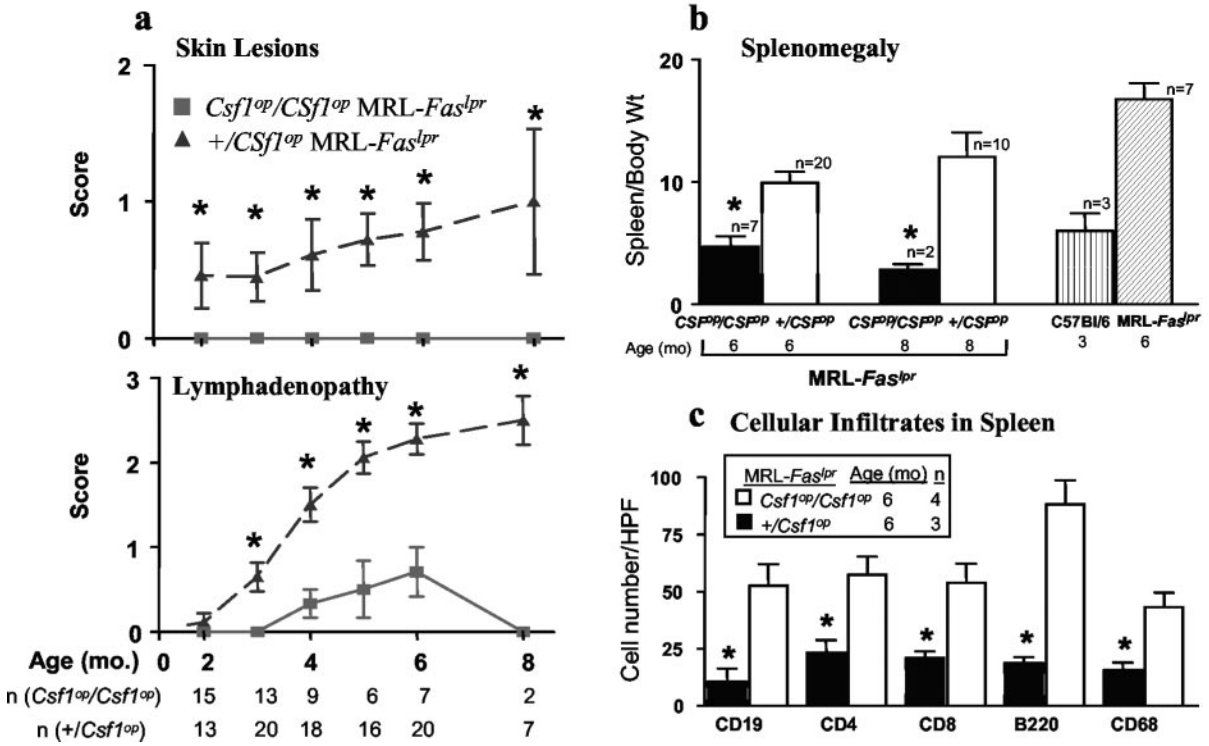

FIGURE 7. Skin lesions, lymphadenopathy, and splenomegaly are suppressed in CSF-1-deficient MRL-*Fas*^{lpr} mice. Skin lesions and lymphadenopathy were assessed from 2 to 8 mo of age (*a* and *c*). Skin lesions were prevented, whereas lymphadenopathy was suppressed in the CSF-1-deficient MRL-*Fas*^{lpr} mice as compared with the CSF-1-intact MRL-*Fas*^{lpr} strain. In addition, the increase in spleen size, characteristic of the MRL-*Fas*^{lpr} strain, did not occur in the spleens of CSF-1-deficient mice (*b*). A reduction in T cells (CD4, CD8, B220), B cells (CD19, B220), and Mϕ (CD68) at 6 mo of age is responsible for the suppressed expansion of spleen size in the CSF-1-deficient as compared with CSF-1-intact MRL-*Fas*^{lpr} mice (*c*). (10,000 cells assessed). Values are means ± SE; ∗, $p \leq 0.05$, *Csf1*^{op}/*Csf1*^{op} vs +/*Csf1*^{op} MRL-*Fas*^{lpr} mice.

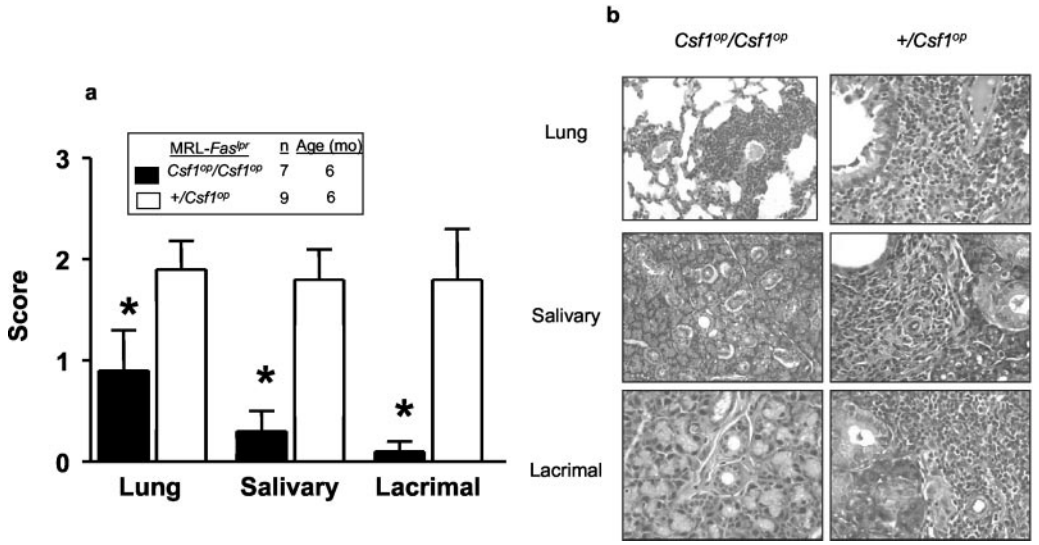

FIGURE 8. Lung, and salivary and lacrimal gland infiltrates are suppressed in CSF-1-deficient mice. Tissues are compared in CSF-1-deficient and CSF-1-intact MRL-*Fas*^{lpr} mice (*a*), representative photomicrographs (*b*). Note the cellular infiltration in CSF-1-intact MRL-*Fas*^{lpr} lungs, and salivary and lacrimal glands as compared with corresponding tissues from the CSF-1-deficient MRL-*Fas*^{lpr} mice. Values are means ± SE; ∗, $p \leq 0.05$, *Csf1*^{op}/*Csf1*^{op} vs +/*Csf1*^{op} MRL-*Fas*^{lpr} mice. Magnification = ×400.

(21 day of age) as compared with age-matched CSF-1-intact MRL-*Fas*^{lpr} mice (Fig. 10). Because CSF-1 improves B cell survival in the MRL-*Fas*^{lpr} and normal strains (48), the absence of CSF-1 in the CSF-1-deficient MRL-*Fas*^{lpr} strain may lead to a decrease in B cells and account for the suppression of circulating autoantibodies.

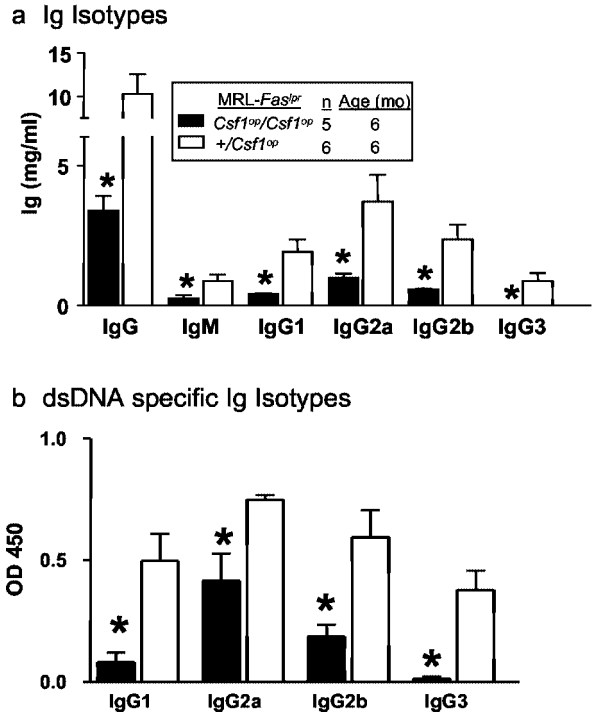

FIGURE 9. Suppressed serum total IgG, IgM, and IgG isotypes (IgG1, IgG2a, IgG2b, and IgG3) in CSF-1-deficient as compared with CSF-1-intact MRL-*Fas*^{lpr} mice (6 mo of age) (*a*). Similarly, the dsDNA specific Ig isotype (IgG1, IgG2a, IgG2b, and IgG3) levels were diminished in the CSF-1-deficient MRL-*Fas*^{lpr} strains. Igs determined by ELISA. Values are means ± SE; ∗, $p \leq 0.05$, *Csf1*^{op}/*Csf1*^{op} vs +/*Csf1*^{op} MRL-*Fas*^{lpr} mice.

Discussion

The present study indicates that CSF-1 is instrumental in the pathogenesis of lupus nephritis and other tissues targeted for autoimmune injury in the MRL-*Fas*^{lpr} strain. CSF-1-deficient MRL-*Fas*^{lpr} mice are protected from nephritis, and pathology in the systemic tissue (skin, lungs, lacrimal and salivary glands, lymphadenopathy and splenomegaly) as compared with the CSF-1-intact MRL-*Fas*^{lpr} strain. The extensive accumulation of Mϕ and T cells into the interstitium, glomerulus, and perivascular regions of the kidney, and in the lung, lacrimal and salivary glands, and spleen is dramatically suppressed in CSF-1-deficient MRL-*Fas*^{lpr} strain as compared with the wild-type strain. Minimal renal histopathology in CSF-1-deficient MRL-*Fas*^{lpr} mice is accompanied by reduced indices of injury and repair including TEC apoptosis and proliferation and nephritogenic chemokines/cytokines. In addition, there is a decrease in circulating Ig isotypes and dsDNA autoantibody isotypes and a reduction in Ig deposits in the renal glomeruli in CSF-1-deficient MRL-*Fas*^{lpr} mice. This suggests that at least some autoantibodies in the CSF-1-intact mice are dependent on CSF-1. Taken together, CSF-1 mediates a broad spectrum of leukocyte functions that contribute to the pathogenesis of autoimmune disease in the MRL-*Fas*^{lpr} strain.

CSF-1 regulates many biologic functions. CSF-1-deficient mice have a reduction in tissue Mϕ in most tissues, are osteopetrotic (due to a paucity of osteoclasts), toothless, poorly fertile, and have a low body weight (17, 50–52). The reduced body weight and size of the CSF-1-deficient MRL-*Fas*^{lpr} strain is related to their smaller skeletal frame that is secondary to abnormal skeletal development. Although CSF-1-deficient MRL-*Fas*^{lpr} and CSF-1-deficient mice on an outbred background have a higher mortality than wild-type mice (53), the vast majority of deaths occur within the first month of life and are probably related to skeletal disorders and postweaning adaptation. A similar situation exists on the FVB/NJ background (E. R. Stanley, unpublished observations). Thus, the CSF-1-deficient mice surviving beyond 1 mo, like those used in this study, are quite healthy. For example, CSF-1-deficient mice have normal T cell-dependent and -independent immune responses (54), and the bone marrow cellularity and the osteopetrotic condition

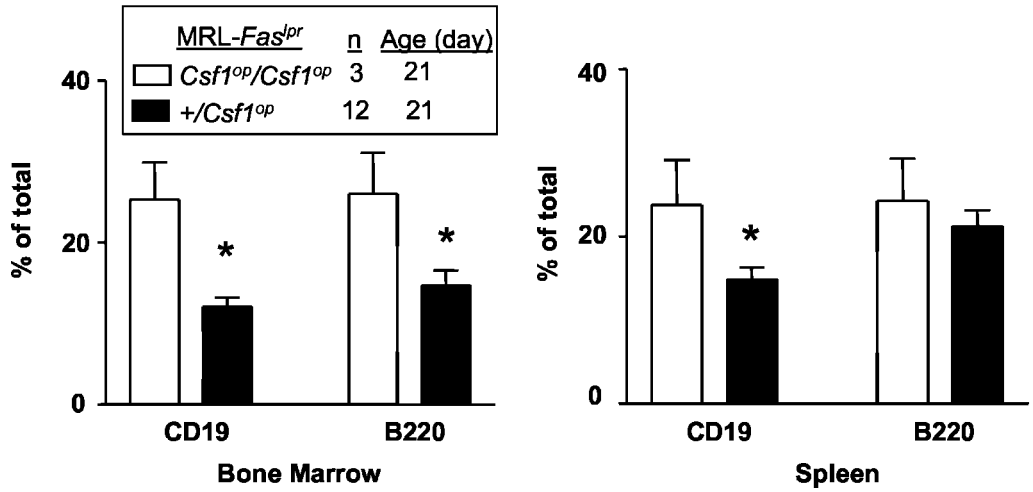

FIGURE 10. B cell apoptosis is increased in CSF-1-deficient MRL-*Fas*^{lpr} mice. B cell apoptosis is increased in the bone marrow and spleen in CSF-1-deficient as compared with CSF-1-intact MRL-*Fas*^{lpr} mice (21 day of age). Values are means ± SE; ∗, $p \leq 0.05$, *Csf1*^{op}/*Csf1*^{op} vs +/*Csf1*^{op} MRL-*Fas*^{lpr} mice.

largely recovers by 7 mo of life (55). Therefore, the difference in the phenotype of CSF-1-deficient and CSF-1-intact MRL-*Fas*^{lpr} strains is not the result of poor health.

Renal disease in the MRL-*Fas*^{lpr} mice is dependent on infiltrating leukocytes. During renal inflammation induced by ligating the ureter, CSF-1 mediates inflammation and tissue injury(s). We have previously shown that a central mechanism responsible for tissue injury is that following activation, Mϕ mediate renal resident cell apoptosis (7). In this model, CSF-1 is responsible for multiple steps leading to Mϕ mediated TEC apoptosis, including 1) Mϕ recruitment, 2) Mϕ survival and proliferation, and 3) enhancement of Mϕ activation (6). Particularly striking in the present study is the paucity of Mϕ and T cells that accumulate in the CSF-1-deficient MRL-*Fas*^{lpr} kidneys as compared with the wild-type strain. We suggest that a primary mechanism responsible for the intrarenal accumulation of Mϕ and T cells is CSF-1-mediated recruitment of leukocytes. We showed previously that implantation of TEC constitutively expressing CSF-1 under the renal capsule fosters an influx of Mϕ followed by T cells into the kidney adjacent to the implant in *Fas*^{lpr} strains, and initiates nephritis (15). Thus, it follows that in MRL-*Fas*^{lpr} mice lacking CSF-1, there is a failure to recruit Mϕ and T cells into the kidney. In fact, the striking reduction of Mϕ and T cells in the MRL-*Fas*^{lpr} kidney is reminiscent of the protection from leukocytic accumulation in the MCP-1-deficient MRL-*Fas*^{lpr} strain. In the MCP-1-deficient MRL-*Fas*^{lpr} mice the accumulation of Mϕ and T cells in the MRL-*Fas*^{lpr} kidney is almost totally suppressed. Because MCP-1 recruits these leukocytes, but does not regulate proliferation, activation or survival, failed recruitment is totally responsible for the paucity of leukocytes in MCP-1-deficient MRL-*Fas*^{lpr} kidneys (23). Thus, CSF-1 and MCP-1 are each necessary, but not sufficient, to recruit leukocytes into the kidney.

Although CSF-1 recruits leukocytes, it is also responsible for intrarenal leukocytic proliferation because we detected a decrease in the percentage of proliferating mononuclear cell infiltrates in the CSF-1-deficient MRL-*Fas*^{lpr} as compared with wild-type kidneys. Conversely, there was no difference in the percentage of apoptotic mononuclear cell infiltrates in CSF-1-deficient and wild-type MRL-*Fas*^{lpr} strains. Thus, the survival of leukocytes within the kidney is not altered in CSF-1-deficient MRL-*Fas*^{lpr} mice. Taken together, this evidence supports the concept that CSF-1-dependent intrarenal leukocyte recruitment and proliferation is responsible for fostering an accumulation of Mϕ and T cells in the MRL-*Fas*^{lpr} kidneys. Parenthetically, it is unlikely that the reduction in leukocyte accumulation in the CSF-1-deficient kidneys is a result of fewer circulating monocytes because we detected similar CD68 and white cell counts in CSF-1-deficient and CSF-1-intact MRL-*Fas*^{lpr} strains and by 2 mo of age, the circulating monocyte levels in CSF-1-deficient mice of other strains have been shown to be normal (56). Similarly, whereas the numbers of Mϕ in the kidney during urethal ligation is reduced by treatment with anti-CSF-1 Ab, this reduction is not related to fewer blood monocytes (57). Because the percentage of activated Mϕ is reduced in the CSF-1-deficient vs the wild-type MRL-*Fas*^{lpr} strain, a reduction in activated Mϕ may contribute to diminished Mϕ-mediated CSF-1-dependent renal injury. Of note, Mϕ and T cell accumulation in the CSF-1-deficient MRL-*Fas*^{lpr} kidneys destined to spontaneously develop nephritis, is far less than in CSF-1-deficient nonautoimmune surgically induced (ureteral ligation) nephritis. This suggests that CSF-1-regulated recruitment of Mϕ and T cells, and CSF-1-mediated Mϕ proliferation and activation is more pivotal in initiating and promoting renal disease in the MRL-*Fas*^{lpr} strain, than in other forms of kidney disease. Taken together, our data suggest that CSF-1-mediated Mϕ and T cell recruitment, intrarenal leukocyte proliferation, and Mϕ activation is central to the initiating and mediating renal destruction in the MRL-*Fas*^{lpr} strain.

Previous studies have shown that B cell production is suppressed in CSF-1-deficient mice (48, 49). We now report that CSF-1 directly or indirectly mediates B cells and Ab production in the MRL-*Fas*^{lpr} strain. This is based on the findings that circulating total Ig, Ig isotypes (G1, G2a, G2b, and G3), anti-dsDNA Ab isotypes (G1, G2a, G2b, and G3), and IgG deposits in the kidney are markedly reduced in CSF-1-deficient MRL-*Fas*^{lpr} as compared with wild-type mice. It is likely that in the MRL-*Fas*^{lpr} strain, as in other strains (48, 49), there are fewer B cells in mice lacking CSF-1. We detected increased B cell apoptosis in the bone marrow and spleen in CSF-1-deficient as compared with CSF-1-intact neonatal MRL-*Fas*^{lpr} mice. In addition, we detected a reduction in B cells in the spleens of neonates and aged mice (6 mo of age), and a decrease in B cells in the circulation (data not shown). This suggests that B cell survival and autoantibody production in MRL-*Fas*^{lpr} mice is dependent, at least in part, on CSF-1.

We are not certain whether it is the impact on Mϕ, T cells, and/or B cells that is responsible for suppressing lupus nephritis,

and the systemic illness in the CSF-1-deficient MRL-*Fas*^{lpr} strain. This is because the association of lupus nephritis and Ab deposition are not necessarily linked. For example, MCP-1-deficient MRL-*Fas*^{lpr} mice are spared from the loss of kidney function due to decreased recruitment of leukocytes into the kidney, and yet circulating Abs, and Ig deposits in the kidneys are comparable to those in the MCP-1-intact mice (23). Similarly, renal disease is protected in γ-chain-deficient NZB/NZW F_1 hybrid mice despite comparable Ig deposits in glomeruli as compared with the wild-type control mice (58). In contrast, renal disease is suppressed in B cell- and T cell-deficient MRL-*Fas*^{lpr} mice (59, 60). Thus, the CSF-1-dependent mechanism responsible for suppressing lupus nephritis may involve the cellular and/or humoral arm of the immune response apart from direct effects on the recruitment and proliferation of activated Mϕ.

The present study indicates that CSF-1 has a broad impact on a spectrum of leukocytic functions that mediate lupus nephritis and the systemic illness in the MRL-*Fas*^{lpr} strain. The issue remains, whether blocking CSF-1 in patients with lupus offers a therapeutic strategy to combat disease? CSF-1-deficient mice have numerous deleterious features including skeletal abnormalities and poor fertility. However, these appear to be primarily associated with the requirement of CSF-1 during postnatal development, so that CSF-1 is an attractive therapeutic target. Nevertheless, it is possible that blocking CSF-1 may protect from inflammation but lead to consequences that compromise therapy. With this in mind, it is important to dissect the individual roles of the three different CSF-1 isoforms, the cell surface membrane-spanning glycoprotein, the secreted proteoglycan and the secreted glycoprotein. If a particular CSF-1 isoform is responsible for the initiation and progression of lupus in the MRL-*Fas*^{lpr} strain, more selective therapeutic approaches will be tailored to minimize deleterious consequences.

Acknowledgments

We thank Drs. Katherine J. Moore and Gregory Tesch for their contribution in the initial development of the CSF-1-deficient strains, and Dr. Lisa Zhang for assisting with the genotyping.

References

1. Theofilopoulos, A. N., and F. J. Dixon. 1981. Etiopathogenesis of murine SLE. *Immunol. Rev. 55:179.*
2. Moyer, C. F., J. D. Strandberg, and C. L. Reinisch. 1987. Systemic mononuclear-cell vasculitis in MRL/Mp-*lpr*/*lpr* mice: a histologic and immunocytochemical analysis. *Am. J. Pathol. 127:229.*
3. Carvalho-Pinto, C. E., M. I. Garcia, M. Mellado, J. M. Rodriguez-Frade, J. Martin-Caballero, J. Flores, A. C. Martinez, and D. Balomenos. 2002. Autocrine production of IFN-γ by macrophages controls their recruitment to kidney and the development of glomerulonephritis in MRL/*lpr* mice. *J. Immunol. 169:1058.*
4. Dang-Vu, A. P., D. S. Pisetsky, and J. B. Weinberg. 1987. Functional alterations of macrophages in autoimmune MRL-*lpr*/*lpr* mice. *J. Immunol. 138:1757.*
5. Kelley, V. E., and J. B. Roths. 1982. Increase in macrophage Ia expression in autoimmune mice: role of the Ipr gene. *J. Immunol. 129:923.*
6. Lenda, D. M., E. Kikawada, E. R. Stanley, and V. R. Kelley. 2003. Reduced macrophage recruitment, proliferation, and activation in colony-stimulating factor-1-deficient mice results in decreased tubular apoptosis during renal inflammation. *J. Immunol. 170:3254.*
7. Tesch, G. H., A. Schwarting, K. Kinoshita, H. Y. Lan, B. J. Rollins, and V. R. Kelley. 1999. Monocyte chemoattractant protein-1 promotes macrophage-mediated tubular injury, but not glomerular injury, in nephrotoxic serum nephritis. *J. Clin. Invest. 103:73.*
8. Stanley, E. R. 2000. CSF-1. In *Cytokine Reference: A Compendium of Cytokines and Other Mediators of Host Defense.* M. F. J. J Oppenheim, ed. Academic Press, London, p. 911.
9. Praloran, V. 1991. Structure, biosynthesis and biological roles of monocyte-macrophage colony stimulating factor (CSF-1 or M-CSF). *Nouv. Rev. Fr. Hematol. 33:323.*
10. Kamanna, V. S., R. Pai, B. Bassa, and M. A. Kirschenbaum. 1996. Activation of mesangial cells with TNF-α stimulates M-CSF gene expression and monocyte proliferation: evidence for involvement of protein kinase C and protein tyrosine kinase. *Biochim. Biophys. Acta 1313:161.*
11. Yui, M. A., W. H. Brissette, D. C. Brennan, R. P. Wuthrich, and V. E. Rubin-Kelley. 1991. Increased macrophage colony-stimulating factor in neonatal and adult autoimmune MRL-*lpr* mice. *Am. J. Pathol. 139:255.*
12. Naito, T., R. C. Griffiths, T. M. Coffman, and V. R. Kelley. 1996. Transplant approach establishes that kidneys are responsible for serum CSF-1 but require a stimulus in MRL-*lpr* mice. *Kidney Int. 49:67.*
13. Wada, T., T. Naito, R. C. Griffiths, T. M. Coffman, and V. R. Kelley. 1997. Systemic autoimmune nephritogenic components induce CSF-1 and TNF-α in MRL kidneys. *Kidney Int. 52:934.*
14. Brennan, D. C., A. M. Jevnikar, R. D. Bloom, W. H. Brissette, G. G. Singer, and V. R. Kelley. 1992. Cultured mesangial cells from autoimmune MRL-*lpr* mice have decreased secreted and surface M-CSF. *Kidney Int. 42:279.*
15. Naito, T., H. Yokoyama, K. J. Moore, G. Dranoff, R. C. Mulligan, and V. R. Kelley. 1996. Macrophage growth factors introduced into the kidney initiate renal injury. *Mol. Med. 2:297.*
16. Marks, S. C., Jr., and P. W. Lane. 1976. Osteopetrosis, a new recessive skeletal mutation on chromosome 12 of the mouse. *J. Hered. 67:11.*
17. Wiktor-Jedrzejczak, W., A. Bartocci, A. W. Ferrante, Jr., A. Ahmed-Ansari, K. W. Sell, J. W. Pollard, and E. R. Stanley. 1990. Total absence of colony-stimulating factor 1 in the macrophage-deficient osteopetrotic (*op*/*op*) mouse. *Proc. Natl. Acad. Sci. USA 87:4828.*
18. Yoshida, H., S. Hayashi, T. Kunisada, M. Ogawa, S. Nishikawa, H. Okamura, T. Sudo, and L. D. Shultz. 1990. The murine mutation osteopetrosis is in the coding region of the macrophage colony stimulating factor gene. *Nature 345:442.*
19. Pollard, J. W., J. S. Hunt, W. Wiktor-Jedrzejczak, and E. R. Stanley. 1991. A pregnancy defect in the osteopetrotic (*op*/*op*) mouse demonstrates the requirement for CSF-1 in female fertility. *Dev. Biol. 148:273.*
20. Cohen, P. E., O. Chisholm, R. J. Arceci, E. R. Stanley, and J. W. Pollard. 1996. Absence of colony-stimulating factor-1 in osteopetrotic (*csfmop*/*csfmop*) mice results in male fertility defects. *Biol. Reprod. 55:310.*
21. Ryan, G. R., X. M. Dai, M. G. Dominguez, W. Tong, F. Chuan, O. Chisholm, R. G. Russell, J. W. Pollard, and E. R. Stanley. 2001. Rescue of the colony-stimulating factor 1 (CSF-1)-nullizygous mouse (*Csf1*^{op}/*Csf1*^{op}) phenotype with a CSF-1 transgene and identification of sites of local CSF-1 synthesis. *Blood 98:74.*
22. Schwarting, A., T. Wada, K. Kinoshita, G. Tesch, and V. R. Kelley. 1998. IFN-γ receptor signaling is essential for the initiation, acceleration, and destruction of autoimmune kidney disease in MRL-*Fas*^{lpr} mice. *J. Immunol. 161:494.*
23. Tesch, G. H., S. Maifert, A. Schwarting, B. J. Rollins, and V. R. Kelley. 1999. Monocyte chemoattractant protein 1-dependent leukocytic infiltrates are responsible for autoimmune disease in MRL-*Fas*^{lpr} mice. *J. Exp. Med. 190:1813.*
24. Kinoshita, K., G. Tesch, A. Schwarting, R. Maron, A. H. Sharpe, and V. R. Kelley. 2000. Costimulation by B7-1 and B7-2 is required for autoimmune disease in MRL-*Fas*^{lpr} mice. *J. Immunol. 164:6046.*
25. Vidal, S., D. H. Kono, and A. N. Theofilopoulos. 1998. Loci predisposing to autoimmunity in MRL-*Fas*^{lpr} and C57BL/6-*Fas*^{lpr} mice. *J. Clin. Invest. 101:696.*
26. Kikawada, E., D. M. Lenda, and V. R. Kelley. 2003. IL-12 deficiency in MRL-*Fas*^{lpr} mice delays nephritis and intrarenal IFN-γ expression, and diminishes systemic pathology. *J. Immunol. 170:3915.*
27. Moore, K. J., T. Naito, C. Martin, and V. R. Kelley. 1996. Enhanced response of macrophages to CSF-1 in autoimmune mice: a gene transfer strategy. *J. Immunol. 157:433.*
28. Schwarting, A., K. Moore, T. Wada, G. Tesch, H. J. Yoon, and V. R. Kelley. 1998. IFN-γ limits macrophage expansion in MRL-*Fas*^{lpr} autoimmune interstitial nephritis: a negative regulatory pathway. *J. Immunol. 160:4074.*
29. Schwarting, A., G. Tesch, K. Kinoshita, R. Maron, H. L. Weiner, and V. R. Kelley. 1999. IL-12 drives IFN-γ-dependent autoimmune kidney disease in MRL-*Fas*^{lpr} mice. *J. Immunol. 163:6884.*
30. O'Connor, K. C., K. Nguyen, and B. D. Stollar. 2001. Recognition of DNA by V_H and F_v domains of an IgG anti-poly(dC) antibody with a singly mutated V_H domain. *J. Mol. Recognit. 14:18.*
31. Sobel, E. S., T. Katagiri, K. Katagiri, S. C. Morris, P. L. Cohen, and R. A. Eisenberg. 1991. An intrinsic B cell defect is required for the production of autoantibodies in the *lpr* model of murine systemic autoimmunity. *J. Exp. Med. 173:1441.*
32. Santoro, T. J., J. P. Portanova, and B. L. Kotzin. 1988. The contribution of L3T4$^+$ T cells to lymphoproliferation and autoantibody production in MRL-*lpr*/*lpr* mice. *J. Exp. Med. 167:1713.*
33. Merino, R., M. Iwamoto, L. Fossati, and S. Izui. 1993. Polyclonal B cell activation arises from different mechanisms in lupus- prone (NZB × NZW)F_1 and MRL/MpJ-*lpr*/*lpr* mice. *J. Immunol. 151:6509.*
34. Moore, K. J., T. Wada, S. D. Barbee, and V. R. Kelley. 1998. Gene transfer of RANTES elicits autoimmune renal injury in MRL-*Fas*^{lpr} mice. *Kidney Int. 53:1631.*
35. Haas, C., B. Ryffel, and M. Le Hir. 1997. IFN-γ is essential for the development of autoimmune glomerulonephritis in MRL/*lpr* mice. *J. Immunol. 158:5484.*
36. Yokoyama, H., B. Kreft, and V. R. Kelley. 1995. Biphasic increase in circulating and renal TNF-α in MRL-*lpr* mice with differing regulatory mechanisms. *Kidney Int. 47:122.*
37. Bonventre, J. V. 2003. Dedifferentiation and proliferation of surviving epithelial cells in acute renal failure. *J. Am. Soc. Nephrol. 14(Suppl. 1):S55.*
38. Sheridan, A. M., and J. V. Bonventre. 2001. Pathophysiology of ischemic acute renal failure. *Contrib. Nephrol. 132:7.*
39. Cohen, P. L., and R. A. Eisenberg. 1992. The *lpr* and *gld* genes in systemic autoimmunity: life and death in the *Fas* lane. *Immunol. Today 13:427.*
40. Watanabe, D., T. Suda, H. Hashimoto, and S. Nagata. 1995. Constitutive activation of the Fas ligand gene in mouse lymphoproliferative disorders. *EMBO J. 14:12.*
41. Mike, A., N. Nagaoka, Y. Tagami, M. Miyashita, S. Shimada, K. Uchida, M. Nanno, and M. Ohwaki. 1999. Prevention of B220$^+$ T cell expansion and

prolongation of lifespan induced by *Lactobacillus casei* in MRL/*lpr* mice. *Clin. Exp. Immunol. 117:368*.
42. Muller, M., A. Emmendorffer, and M. L. Lohmann-Matthes. 1991. Expansion and high proliferative potential of the macrophage system throughout life time of lupus-prone NZB/W and MRL *lpr*/*lpr* mice: lack of down-regulation of extramedullar macrophage proliferation in the postnatal period. *Eur. J. Immunol. 21:2211*.
43. Pineda, L. L., A. Nakano, M. Iijima, M. Wada, Y. Yamasaki, and T. Harada. 2003. A new mutation, ataxia and male sterility (ams), of autoimmune-prone MRL/*lpr* mouse is not linked to *lpr* gene but associated with reduction of spleen size and alteration of lymphocyte subpopulations. *Pathol. Int. 53:390*.
44. William, J., C. Euler, S. Christensen, and M. J. Shlomchik. 2002. Evolution of autoantibody responses via somatic hypermutation outside of germinal centers. *Science 297:2066*.
45. Hoffman, R. W., M. A. Alspaugh, K. S. Waggie, J. B. Durham, and S. E. Walker. 1984. Sjogren's syndrome in MRL/*l* and MRL/*n* mice. *Arthritis Rheum. 27:157*.
46. Andrews, B. S., R. A. Eisenberg, A. N. Theofilopoulos, S. Izui, C. B. Wilson, P. J. McConahey, E. D. Murphy, J. B. Roths, and F. J. Dixon. 1978. Spontaneous murine lupus-like syndromes: clinical and immunopathological manifestations in several strains. *J. Exp. Med. 148:1198*.
47. Shlomchik, M. J., M. P. Madaio, D. Ni, M. Trounstein, and D. Huszar. 1994. The role of B cells in *lpr*/*lpr*-induced autoimmunity. *J. Exp. Med. 180:1295*.
48. Lu, L., and D. G. Osmond. 2001. Regulation of cell survival during B lymphopoiesis in mouse bone marrow: enhanced pre-B-cell apoptosis in CSF-1-deficient *op*/*op* mutant mice. *Exp. Hematol. 29:596*.
49. Tagaya, H., T. Kunisada, H. Yamazaki, T. Yamane, T. Tokuhisa, E. F. Wagner, T. Sudo, L. D. Shultz, and S. I. Hayashi. 2000. Intramedullary and extramedullary B lymphopoiesis in osteopetrotic mice. *Blood 95:3363*.
50. Cecchini, M. G., M. G. Dominguez, S. Mocci, A. Wetterwald, R. Felix, H. Fleisch, O. Chisholm, W. Hofstetter, J. W. Pollard, and E. R. Stanley. 1994. Role of colony stimulating factor-1 in the establishment and regulation of tissue macrophages during postnatal development of the mouse. *Development 120:1357*.
51. Felix, R., M. G. Cecchini, W. Hofstetter, P. R. Elford, A. Stutzer, and H. Fleisch. 1990. Impairment of macrophage colony-stimulating factor production and lack of resident bone marrow macrophages in the osteopetrotic *op*/*op* mouse. *J. Bone Miner. Res. 5:781*.
52. Wiktor-Jedrzejczak, W. W., A. Ahmed, C. Szczylik, and R. R. Skelly. 1982. Hematological characterization of congenital osteopetrosis in *op*/*op* mouse: possible mechanism for abnormal macrophage differentiation. *J. Exp. Med. 156:1516*.
53. Dai, X. M., G. R. Ryan, A. J. Hapel, M. G. Dominguez, R. G. Russell, S. Kapp, V. Sylvestre, and E. R. Stanley. 2002. Targeted disruption of the mouse colony-stimulating factor 1 receptor gene results in osteopetrosis, mononuclear phagocyte deficiency, increased primitive progenitor cell frequencies, and reproductive defects. *Blood 99:111*.
54. Chang, M. D., E. R. Stanley, H. Khalili, O. Chisholm, and J. W. Pollard. 1995. Osteopetrotic (*op*/*op*) mice deficient in macrophages have the ability to mount a normal T-cell-dependent immune response. *Cell Immunol. 162:146*.
55. Begg, S. K., J. M. Radley, J. W. Pollard, O. T. Chisholm, E. R. Stanley, and I. Bertoncello. 1993. Delayed hematopoietic development in osteopetrotic (*op*/*op*) mice. *J. Exp. Med. 177:237*.
56. Dai, X. M., X. H. Zong, V. Sylvestre, and E. R. Stanley. 2004. Incomplete restoration of colony-stimulating factor 1 (CSF-1) function in CSF-1-deficient *Csf1op*/*Csf1op* mice by transgenic expression of cell surface CSF-1. *Blood 103:1114*.
57. Le Meur, Y., G. H. Tesch, P. A. Hill, W. Mu, R. Foti, D. J. Nikolic-Paterson, and R. C. Atkins. 2002. Macrophage accumulation at a site of renal inflammation is dependent on the M-CSF/c-*fms* pathway. *J. Leukocyte Biol. 72:530*.
58. Clynes, R., C. Dumitru, and J. V. Ravetch. 1998. Uncoupling of immune complex formation and kidney damage in autoimmune glomerulonephritis. *Science 279:1052*.
59. Wada, T., A. Schwarting, M. S. Chesnutt, D. Wofsy, and V. Rubin Kelley. 2001. Nephritogenic cytokines and disease in MRL-*Fas*^{lpr} kidneys are dependent on multiple T-cell subsets. *Kidney Int. 59:565*.
60. Chan, O. T., M. P. Madaio, and M. J. Shlomchik. 1999. B cells are required for lupus nephritis in the polygenic, *Fas*-intact MRL model of systemic autoimmunity. *J. Immunol. 163:3592*.